

Rotating scalarized black holes in scalar couplings to two topological terms

De-Cheng Zou^{a*} and Yun Soo Myung^{b†}

^aCenter for Gravitation and Cosmology and College of Physical Science and Technology,
Yangzhou University, Yangzhou 225009, China

^bInstitute of Basic Sciences and Department of Computer Simulation, Inje University
Gimhae 50834, Korea

Abstract

The tachyonic instability of the Kerr black holes is analyzed in the Einstein-scalar theory with the quadratic scalar couplings to two topological terms which are parity-even Gauss-Bonnet and parity-odd Chern-Simons terms. For positive coupling α , we use the (2+1)-dimensional hyperboloidal foliation method to derive the threshold curve which is the boundary between stable and unstable Kerr black holes by considering a spherically symmetric scalar-mode perturbation. In case of negative coupling, a newly bound of $a \geq 0.26$ with a the rotation parameter is found for unstable Kerr black holes and its threshold curve is derived.

*e-mail address: dczou@yzu.edu.cn

†e-mail address: ysmjung@inje.ac.kr

1 Introduction

Black hole scalarization is well understood as a good mechanism to have a black hole with scalar hair. When a scalar field couples to either Gauss-Bonnet term [1, 2, 3] or to Maxwell term [4], the tachyonic instability for general relativity (GR) black holes represents the hallmark of the spontaneous scalarization. As the linear instability develops and the scalar field grows, nonlinear terms play the important role and quench the instability. Eventually, the scalarized black hole solutions are constructed numerically as infinite $n = 0, 1, 2, \dots$ black holes where the fundamental ($n = 0$) scalarized black hole is stable against radial perturbations whereas radially excited black holes with $n > 0$ turn out to be unstable, irrespective of coupling terms [5]. This implies that the fundamental scalarized black hole is considered as an endpoint of the GR black hole.

Now, we wish to mention briefly the onset of scalarization for rotating GR black holes. Spontaneous scalarization of Kerr black holes has been firstly studied in a scalar coupling to the Gauss-Bonnet term with positive coupling [6, 7], implying that the high rotation with $a \geq 0.5$ suppresses scalarization. Recently, an a -bound of $a/M \geq 0.5$ (high rotation) was found as the onset of scalarization for Kerr black holes with negative coupling [8]. It implies that there is a minimum rotation $a_{\min}/M = 0.5$ below which the instability never appears. This a -bound was recovered analytically in [9] and numerically in [10]. In this direction, the spin-induced scalarized black holes were numerically constructed for the high rotation and negative coupling [11, 12].

On the other hand, it is found that no such an a -bound exists when investigating the tachyonic instability of Kerr black holes in a scalar coupling to the Chern-Simons term with negative coupling [13]. This suggests that the odd-parity Chern-Simons term plays a different role from the even-parity Gauss-Bonnet term.

In this work, we wish to perform the instability analysis of the Kerr black holes in scalar couplings to two topological terms with the same quadratic coupling parameter α . The organization of our work is as follows. In section 2, we mention Kerr black holes without scalar hair in the Einstein-scalar-Gauss-Bonnet-Chern-Simons (EsGBCS) theory. We discuss the tachyonic instability of Kerr black holes for both positive and negative α in section 3. It is essential to derive the time evolution of a spherically symmetric scalar mode ($l = m = 0$) for the instability analysis because the Kerr background is a stationary, axisymmetric, and non-static spacetime.

We will use the (2+1)-dimensional hyperboloidal foliation method to derive the time evolution of a spherically symmetric scalar-mode. It will take a long time to complete the computations even though we confine ourselves to a spherically symmetric scalar-mode. For positive α , we wish to derive the threshold curve which is the boundary between stable and unstable Kerr black holes. Curiously, we expect to obtain a different a -bound of $a \geq 0.26$, in addition to the threshold curve, for negative α . In section 4, we will discuss our results by comparing with those of slowly rotating black holes in the EsGBCS theory.

2 Kerr black holes

Here, we consider the action of Einstein-scalar-Gauss-Bonnet-Chern-Simons (EsGBCS) theory [14] as

$$S_{\text{EsGBCS}} = \frac{1}{16\pi} \int d^4x \sqrt{-g} \left[R - \frac{1}{2}(\partial\phi)^2 + f(\phi)(R_{\text{GB}}^2 + {}^*RR) \right], \quad (1)$$

where we use geometric units of $G = c = 1$. ϕ is a real scalar field and $f(\phi)$ is the coupling function coupled to two topological terms: the Gauss-Bonnet term $R_{\text{GB}}^2 = R^2 - 4R_{\mu\nu}R^{\mu\nu} + R_{\mu\nu\rho\sigma}R^{\mu\nu\rho\sigma}$ and the Chern-Simons term ${}^*RR = \frac{1}{2}\epsilon^{\mu\nu\rho\sigma}R^\eta_{\xi\rho\sigma}R^\xi_{\eta\mu\nu}$. Here we choose the quadratic coupling function of $f(\phi) = \alpha\phi^2$ because it provides the simplicity for spontaneous scalarization. To allow for spontaneous scalarization, the coupling function $f(\phi)$ should possess certain properties. The GR (Kerr) black hole solutions should remain solutions of the theory. This is the case when the Gauss-Bonnet and Chern-Simons terms do not contribute to the field equations. Selecting a coupling function $f(\phi)$ such that $f'(\phi) = 0$ for $\phi = 0$, the source term in the scalar equation of $\nabla^2\phi + f'(\phi)(R_{\text{GB}}^2 + {}^*RR) = 0$ vanishes for $\phi = 0$. It implies that $\phi = 0$ is a solution. This is why we choose a non-minimally coupling function $f(\phi)$. In this direction, a linear function of $f(\phi) = \alpha\phi$ is excluded. Also, if one chooses no scalar coupling like $f(\phi) = \alpha$, the Gauss-Bonnet and Chern-Simons terms do not contribute to the field equations absolutely because they are topological terms.

Firstly, we derive the Einstein equation

$$G_{\mu\nu} = \frac{1}{2}\partial_\mu\phi\partial_\nu\phi - \frac{1}{4}g_{\mu\nu}(\partial\phi)^2 - \alpha\phi^2 H_{\mu\nu} - 4\alpha[\nabla^\rho\nabla^\sigma(\phi^2)P_{\mu\rho\nu\sigma} + C_{\mu\nu}], \quad (2)$$

where $H_{\mu\nu}$ and $P_{\mu\rho\nu\sigma}$ take the forms

$$H_{\mu\nu} = 2(RR_{\mu\nu} - 2R_{\mu\rho}R^{\rho}{}_{\nu} - 2R^{\rho\sigma}R_{\mu\rho\nu\sigma} + R_{\mu}{}^{\rho\sigma\lambda}R_{\nu\rho\sigma\lambda}) - \frac{1}{2}g_{\mu\nu}R_{\text{GB}}^2, \quad (3)$$

$$P_{\mu\rho\nu\sigma} = R_{\mu\rho\nu\sigma} + g_{\mu\sigma}R_{\nu\rho} - g_{\mu\nu}R_{\rho\sigma} + g_{\nu\rho}R_{\mu\sigma} - g_{\rho\sigma}R_{\mu\nu} + \frac{R}{2}(g_{\mu\nu}g_{\rho\sigma} - g_{\mu\sigma}g_{\nu\rho}). \quad (4)$$

If $f(\phi) = \alpha$, $P_{\mu\nu\rho\sigma}$ -term disappears, implying no modifications of the Einstein equation. On the other hand, the Cotton tensor $C_{\mu\nu}$ is given by

$$C_{\mu\nu} = \nabla_{\rho}(\phi^2) \epsilon^{\rho\sigma\gamma}{}_{(\mu} \nabla_{\gamma} R_{\nu)\sigma} + \frac{1}{2} \nabla_{\rho} \nabla_{\sigma}(\phi^2) \epsilon_{(\nu}{}^{\rho\gamma\delta} R^{\sigma}{}_{\mu)\gamma\delta} \quad (5)$$

with $\epsilon_{\mu\nu\rho\sigma}$ being the 4-dimensional Levi-Civita tensor. However, an important scalar equation is found to be

$$\nabla^2\phi + 2\alpha(R_{\text{GB}}^2 + {}^*RR)\phi = 0. \quad (6)$$

Even though the Einstein equation (2) looks like a complicated form, it is easy to find Kerr black holes when choosing a trivial scalar field. Actually, Eq. (2) together with $\bar{\phi} = 0$ reduces to $\bar{R}_{\mu\nu} = 0$ which implies the rotating GR black hole (Kerr spacetime) written in terms of the Boyer-Lindquist coordinates

$$\begin{aligned} ds_{\text{Kerr}}^2 &= \bar{g}_{\mu\nu} dx^{\mu} dx^{\nu} \\ &= -\frac{\Delta}{\rho^2} (dt - a \sin^2 \theta d\varphi)^2 + \frac{\rho^2}{\Delta} dr^2 + \rho^2 d\theta^2 + \frac{\sin^2 \theta}{\rho^2} [adt - (r^2 + a^2)d\varphi]^2, \end{aligned} \quad (7)$$

where

$$\Delta = r^2 - 2Mr + a^2, \quad \rho^2 = r^2 + a^2 \cos^2 \theta \quad (8)$$

with mass M and rotation parameter $a = J/M > 0$. We mention that Eq. (7) describes a stationary, axisymmetric and non-static spacetime because it does not depend on time, it does not depend on ϕ , and it is not invariant under $t \rightarrow -t$. From $\Delta = 0$, one finds outer/inner horizons

$$r_{\pm} = M \left[1 \pm \sqrt{1 - a^2/M^2} \right], \quad (9)$$

while one gets the angular velocity of rotating black hole as $\Omega_{\text{H}} = a/(r_+^2 + a^2)$.

3 Tachyonic instability of Kerr black holes

We wish to study whether there is a regime within which the Kerr black hole solution is unstable against perturbations in the EsGBCS theory. To this end, we have to obtain

the linearized theory by linearizing the Einstein and scalar equations. Introducing two perturbations $(h_{\mu\nu}, \delta\phi)$ around the Kerr background

$$g_{\mu\nu} = \bar{g}_{\mu\nu} + h_{\mu\nu}, \quad \phi = 0 + \delta\phi, \quad (10)$$

the linearized equation to Eq. (2) takes a simple form

$$\delta R_{\mu\nu}(h) = 0 \rightarrow \bar{\nabla}^\gamma \bar{\nabla}_\mu h_{\nu\gamma} + \bar{\nabla}^\gamma \bar{\nabla}_\nu h_{\mu\gamma} - \bar{\nabla}^2 h_{\mu\nu} - \bar{\nabla}_\mu \bar{\nabla}_\nu h = 0. \quad (11)$$

The tensor-stability analysis for the Kerr black hole with Eq. (11) is the same as in the general relativity. It is found that there are no exponentially growing tensor modes propagating around the Kerr background by making use of the null tetrad formalism [15]. Before we proceed, let us consider the Klein-Gordon equation [16]

$$(\bar{\nabla}^2 - \mu^2)\delta\phi = 0 \quad (12)$$

with μ^2 mass squared. This is a linearized equation for the massive scalar propagating around the Kerr background. Reminding the axisymmetric background shown in Eq. (7), it is convenient to separate the scalar into modes

$$\delta\phi(t, r, \theta, \phi) = \sum_{lm} e^{-i\omega t + im\phi} S_{\ell m}(\theta) \mathcal{R}_{\ell m}(r), \quad (13)$$

where $S_{\ell m}(\theta)$ denotes spheroidal harmonics with $-m \leq \ell \leq m$ and $\mathcal{R}_{\ell m}(r)$ represents radial function. We may choose a positive frequency ω of the mode. Plugging Eq. (13) into Eq. (12), the angular and radial (Teukolsky) equations for $S_{\ell m}(\theta)$ and $\mathcal{R}_{\ell m}(r)$ are given by

$$\frac{1}{\sin\theta} \partial_\theta (\sin\theta \partial_\theta S_{\ell m}) + \left[a^2(\omega^2 - \mu^2) \cos^2\theta - \frac{m^2}{\sin^2\theta} + \lambda_{lm} \right] S_{\ell m} = 0, \quad (14)$$

$$\Delta \partial_r (\Delta \partial_r \mathcal{R}_{\ell m}(r)) - [\Delta U - K^2] \mathcal{R}_{\ell m}(r) = 0 \quad (15)$$

with $U = \mu^2(r^2 + a^2) - 2am\omega + \lambda_{lm}$ and $K = \omega(r^2 + a^2) - am$. Here λ_{lm} is the separation constant given by

$$\lambda_{lm} = l(l+1) + \sum_{k=1}^{\infty} c_k a^{2k} (\mu^2 - \omega^2)^k \quad (16)$$

for $\omega \simeq M$ only. Introducing the tortoise coordinate r_* defined by $dr_* = \frac{r^2 + a^2}{\Delta} dr$ and $\psi(r) = \sqrt{r^2 + a^2} \mathcal{R}(r)$, the Teukolsky equation takes the Schrödinger form

$$\frac{d^2\psi}{dr_*^2} + [\omega^2 - V(r, \omega)]\psi = 0 \quad (17)$$

$$(18)$$

with the potential

$$\begin{aligned}
V(r, \omega) = \omega^2 & - \frac{3\Delta^2 r^2}{(a^2 + r^2)^4} + \frac{\Delta[\Delta + 2r(r - M)]}{(a^2 + r^2)^3} \\
& + \frac{\Delta\mu^2}{a^2 + r^2} - \left[\omega - \frac{am}{a^2 + r^2} \right]^2 \\
& - \frac{\Delta}{(a^2 + r^2)^2} \left[2am\omega + a^2(\mu^2 - \omega^2) - \lambda_{lm} \right]. \tag{19}
\end{aligned}$$

This potential is chosen for studying the superradiant instability [17]. In order to find if there exists a trapping potential (a necessary condition for superradiant instability), one should analyze the shape of potential $V(r, \omega)$ carefully.

Now let us go back to the linearized scalar theory in the EsGBCS theory. The instability of Kerr black holes will be determined by the linearized scalar equation whose form is given by

$$\left(\bar{\nabla}^2 - \mu_{\text{eff}}^2 \right) \delta\phi = 0 \tag{20}$$

with an effective mass

$$\mu_{\text{eff}}^2 \equiv \mu_{\text{GB}}^2 + \mu_{\text{CS}}^2 = -2\alpha \bar{R}_{\text{GB}}^2 - 2\alpha {}^* \bar{R} \bar{R}. \tag{21}$$

Here, we have

$$\bar{R}_{\text{GB}}^2 = \frac{48M^2(r^6 - 15r^4 a^2 \cos^2 \theta + 15r^2 a^4 \cos^4 \theta - a^6 \cos^6 \theta)}{(r^2 + a^2 \cos^2 \theta)^6} \tag{22}$$

$$\simeq \frac{48M^2}{r^6} \left(1 - \frac{21a^2 \cos^2 \theta}{r^2} + \dots \right) \tag{23}$$

and

$${}^* \bar{R} \bar{R} = \frac{96rM^2 a \cos \theta (3r^4 - 10r^2 a^2 \cos^2 \theta + 3a^4 \cos^4 \theta)}{(r^2 + a^2 \cos^2 \theta)^6} \tag{24}$$

$$\simeq \frac{288M^2 a \cos \theta}{r^7} \left(1 - \frac{28a^2 \cos^2 \theta}{3r^2} + \dots \right). \tag{25}$$

Under the parity transformation, one finds that even: $\bar{R}_{\text{GB}}^2(\pi - \theta) \rightarrow \bar{R}_{\text{GB}}^2(\theta)$ and odd: ${}^* \bar{R} \bar{R}(\pi - \theta) \rightarrow -{}^* \bar{R} \bar{R}(\theta)$. At this stage, we mention that Eqs. (23) and (25) represent series forms written in terms of a . In the slowly rotating black holes with $a \ll 1$, one considers the first terms in Eqs. (23) and (25) only [14]. It is important to note that μ_{GB}^2 (μ_{CS}^2) is odd (even) under a combined transformation of $\alpha \rightarrow -\alpha$ and $\theta \rightarrow \pi - \theta$. This implies that positive and negative α will show different results. From now on, we consider two cases of $\alpha > 0$ and $\alpha < 0$ separately.

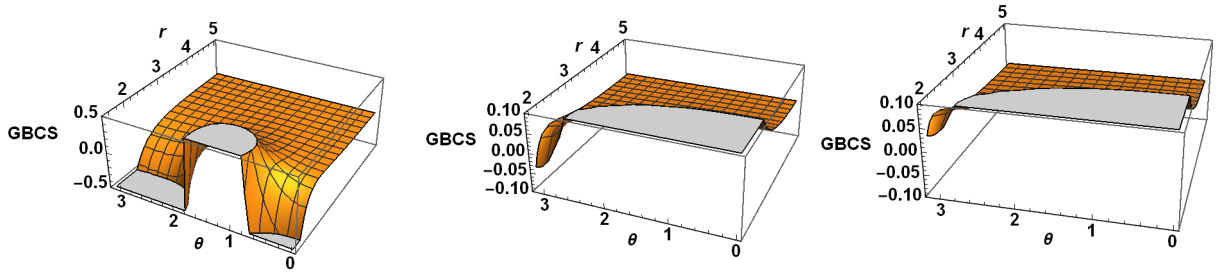


Figure 1: Three 3D graphs for $\text{GBCS}(=\bar{R}_{\text{GB}}^2+{}^*\bar{R}\bar{R})$ with $M = 1$. These include $r \in [r_+, 5]$ and $\theta \in [0, \pi]$. Left: a graph for $a = 0.87$ indicating positive region with negative regions around the poles of $\theta = 0, \pi$. Middle: a graph for $a = 0.27 > 0.26$ representing positive region with a tiny negative region at $\theta = \pi$. Right: a graph for $a = 0.25 < 0.26$ showing whole positive region.

3.1 Positive coupling α

First of all, we note that \bar{R}_{GB}^2 is an even function, while ${}^*\bar{R}\bar{R}$ is an odd function. For $\bar{R}_{\text{GB}}^2 + {}^*\bar{R}\bar{R}(\mu_{\text{eff}}^2$ in Eq.(21)), however, one observes from Fig. 1 that negative (positive) region appears for $a \geq 0.26$. For $a < 0.26$, $\bar{R}_{\text{GB}}^2 + {}^*\bar{R}\bar{R}(\mu_{\text{eff}}^2$ in Eq.(21)) becomes positive (negative) and thus, enhancing scalarization. Our observation comes from \bar{R}_{GB}^2 and ${}^*\bar{R}\bar{R}$ solely but not from including the coupling parameter α . It is well known that the threshold curve $\alpha = \alpha_{\text{th}}(a)$ for Kerr black holes depends on a . However, its form will be determined by performing numerical computations for a long time.

The separation of scalar given by Eq. (13) is impossible to occur here because of $\mu_{\text{eff}}^2(r, \theta, \alpha)$. Instead, we introduce the separation of variables after transforming to the ingoing Kerr-Schild coordinates $\{\tilde{t}, r, \theta, \tilde{\varphi}\}$

$$\delta\phi(\tilde{t}, r, \theta, \tilde{\varphi}) = \frac{1}{r} \sum_m u_m(\tilde{t}, r, \theta) e^{im\tilde{\varphi}}. \quad (26)$$

Plugging Eq. (26) into Eq. (20) leads to the (2+1)-dimensional Teukolsky equation as

$$A^{\tilde{t}\tilde{t}}\partial_{\tilde{t}}^2 u_m + A^{\tilde{t}r}\partial_{\tilde{t}}\partial_r u_m + A^{rr}\partial_r^2 u_m + A^{\theta\theta}\partial_{\theta}^2 u_m + B^{\tilde{t}}\partial_{\tilde{t}} u_m + B^r\partial_r u_m + B^{\theta}\partial_{\theta} u_m + C u_m = 0 \quad (27)$$

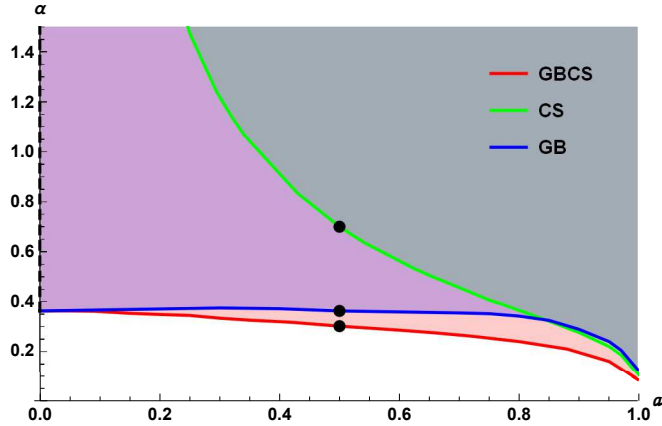


Figure 2: Three threshold curves [$\alpha = \alpha_{\text{th}}(a)$] being the boundary between stable and unstable Kerr black holes by observing time evolution of a $l = m = 0$ -scalar mode for positive α . The GBCS, CS, and GB represent the threshold curves for the presence of Gauss-Bonnet-Chern-Simons, Chern-Simons, and Gauss-Bonnet terms, respectively. Dots (\bullet) represent three different points of $\alpha_{\text{th}} = 0.7$ (CS), 0.363 (GB), and 0.302 (GBCS) at $a = 0.5$. Dashed line ($\alpha \geq 0.363$) on the α -axis is designed for unstable Schwarzschild black holes in the non-rotating limit of $a \rightarrow 0$.

with coefficients

$$\begin{aligned}
 A^{\tilde{t}\tilde{t}} &= \rho^2 + 2Mr, & A^{\tilde{t}r} &= -4Mr, & A^{rr} &= -\Delta, & A^{\theta\theta} &= -1, \\
 B^{\tilde{t}} &= 2M, & B^r &= \frac{2}{r}(a^2 - Mr) - 2ima, & B^\theta &= -\cot\theta, \\
 C &= \frac{m^2}{\sin^2\theta} - \frac{2(a^2 - Mr)}{r^2} + \frac{2ima}{r} + \mu_{\text{eff}}^2 \rho^2.
 \end{aligned} \tag{28}$$

We employ the (2+1)-dimensional hyperboloidal foliation method by introducing the compactified radial coordinates R and suitable time coordinates τ [18] to solve Eq. (27) numerically for the CS term [19] and the GB term [20]. Here, it is not necessary to describe this method explicitly because we have already used it to compute the time evolution of a spherically symmetric scalar-mode [13, 14]. The differential equations in R and θ are solved by using the finite difference method and the time (τ) evolution is obtained by adopting the fourth-order Runge-Kutta integrator when computing $u_{lm}(\tau, R, \theta)$. As an initial scalar mode, we may introduce a Gaussian function [$u_{lm}(\tau = 0, R, \theta) \sim Y_{lm}(\theta)e^{-\frac{(R-R_c)^2}{2\sigma^2}}$] with spherical harmonics $Y_{lm}(\theta)$ localized at $R = R_c$ outside the outer horizon. Since the Kerr spacetime is axisymmetric, the mode coupling may occur such that a purely even (odd)

initial multipole l will excite other even (odd) multipoles (denoted by l') with the same m as it evolves. So, one may consider $l = 0$ and $l = 1$ as representative even and odd multipoles with axisymmetric perturbations with $m = 0$ for the GB term [20]. For the CS term [19], the axisymmetric ($m = 0$) and non-axisymmetric ($m \neq 0$) cases were considered. Here, however, we consider a spherically symmetric scalar-mode of $l = m = 0$ only because it needs much computation times to carry out six different cases: for $\alpha > 0$, $\alpha_{\text{th}}^{\text{GB}}(a)$, $\alpha_{\text{th}}^{\text{CS}}(a)$, $\alpha_{\text{th}}^{\text{GBCS}}(a)$ and for $\alpha < 0$, $-\alpha_{\text{th}}^{\text{GB}}(a)$, $-\alpha_{\text{th}}^{\text{CS}}(a)$, $-\alpha_{\text{th}}^{\text{GBCS}}(a)$. Also, the spherically symmetric scalar-mode could be considered as a representative for all scalar modes when performing tachyonic instability analysis of scalar modes around the Kerr black hole [8].

From Fig. 2, we find three threshold curves (existence curves) $\alpha_{\text{th}}(a)$ which are the boundary between stable and unstable regions based on the time evolutions of a scalar mode u_{00} . We note the range of α_{th} : $\alpha_{\text{th}}^{\text{GB}}, \alpha_{\text{th}}^{\text{GBCS}} \in (0, 0.363]$ but $\alpha_{\text{th}}^{\text{CS}} \in (0, \infty)$. The CS-threshold curve decreases rapidly as a increases, while it never hits the α -axis in the non-rotating limit of $a \rightarrow 0$ [13]. On the other hand, the GB-and GBCS-threshold curves start at $\alpha = 0.363$ on the α -axis corresponding to the threshold of unstable Schwarzschild black hole, whereas they decrease slowly as a increases [7]. The unshaded region [$\alpha < \alpha_{\text{th}}(a)$: no growing mode] of each curve represents the stable Kerr black holes, while the shaded region [$\alpha > \alpha_{\text{th}}(a)$: growing mode] denotes the unstable Kerr black holes. We call the latter as ‘ a dependent α -bound’ for onset of rotating scalarization. Also, Fig. 2 includes the stable and unstable (dashed-line: $\alpha \geq 0.363$) Schwarzschild black holes on the α -axis. We observe that the unstable region increases as α_{th} decreases for fixed $a = 0.5$: the largest $\alpha_{\text{th}} = 0.7$ is obtained for the CS term, the medium $\alpha_{\text{th}} = 0.363$ is for the GB term, and the smallest $\alpha_{\text{th}} = 0.302$ is for the GBCS term. This could be read off from the fact that the role of a is critical in Eq. (25), but it is less critical in Eq. (23). It is worth noting that we have $\alpha_{\text{th}}=0.086$ (GBCS), 0.107 (CS), and 0.126 (GB) in the nearly extremal limit of $a = 0.998$.

Concerning the reliability of numerical tests for positive α , our data includes $(a, \alpha) = \{(0.998, 0.107), (0.362, 1.0)\}$ for CS case appeared in [19] and $(a, \alpha) = \{(0, 0.363), (0.3, 0.375), (0.5, 0.363), (0.9, 0.3)\}$ for GB case (when replacing α by 2α) appeared in [20]. Here, we note that the precision and accuracy of the (2+1)-dimensional hyperboloidal foliation method was tested in Refs.[19, 20]. Furthermore, our data of GBCS for $0 \leq a \leq 0.1$ is the nearly

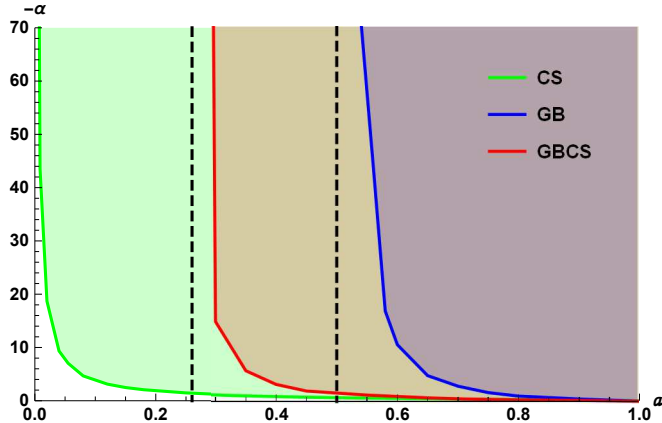


Figure 3: Three threshold curves $[-\alpha = -\alpha_{\text{th}}(a)]$ being the boundary between stable and unstable Kerr black holes by observing time evolution of $l = m = 0$ -scalar mode for negative α . Two dashed lines represent $a = 0.26$ and $a = 0.5$ as minimum values for the a -bound in the GBCS and GB cases, respectively.

same as obtained from a spherically symmetric scalar mode propagating around slowly rotating black holes [14]. Finally, we recover $\alpha_{\text{th}} = 0.363$ for Schwarzschild black hole from GB and GBCS cases when choosing $a = 0$.

3.2 Negative coupling α

We observe from Fig. 1 that a necessary condition for $\bar{R}_{\text{GB}}^2 + {}^* \bar{R} \bar{R} (\mu_{\text{eff}}^2)$ in Eq.(21) to have some negative region is an a -bound of $a \geq 0.26$, enhancing scalarization. The other case of $a < 0.26$ is not allowed for tachyonic instability. From Fig. 3, we confirm that the a -bound for the EsGBCS theory is $a \geq 0.26$, while the a -bound for the EsGB theory denotes $a \geq 0.5$. This implies that an addition of the CS term to the GB term has shifted from the bound of $a \geq 0.5$ to $a \geq 0.26$. We remind the reader that the GBCS and GB are not invariant under the combined transformation of $\theta \rightarrow \pi - \theta$ and $\alpha \rightarrow -\alpha$. So, we have different threshold curves for negative α (Fig. 2) when comparing with positive α (Fig. 3). On the other hand, there is no a -bound for the CS term with negative α . This curve is the same as in Fig. 2 because μ_{CS}^2 is invariant under the combined transformation.

Finally, concerning the reliability of numerical tests for negative α , our data includes $(a, -\alpha) = \{(0.7, 2.9), (0.8, 1.0), (0.9, 0.46)\}$ for GB case (when replacing $-\alpha$ by -2α) appeared in [20].

4 Discussions

First of all, we mention the tachyonic instability for slowly rotating black holes in the EsGBCS theory. It was shown that slowly rotating black holes with $a \ll 1$ are unstable against a spherically symmetric scalar-mode of $l = m = 0$ for positive coupling α only [14]. A threshold curve $\alpha = \alpha_{\text{th}}(a)$ which is the boundary between stable and unstable black holes was derived by considering the constant scalar modes under time evolution. For negative coupling, there is no tachyonic instability for scalarization since the mass term of μ_{eff}^2 is always positive outside the outer horizon. Therefore, any a -bound is not found.

In this work, we have investigated the tachyonic instability for Kerr black holes in the same theory, allowing whole range of $0 \leq a \leq 1$. Since $\mu_{\text{GB}}^2(\mu_{\text{CS}}^2)$ is variant (invariant) under a combined transformation of $\alpha \rightarrow -\alpha$ and $\theta \rightarrow \pi - \theta$, positive and negative α have shown different results. For positive α , we have obtained the threshold curve for the GBCS case (see Fig. 2) which is the nearly same as that for slowly rotating black holes for sufficiently low rotation of $a \ll 1$. On the other hand, for negative α , we have obtained an a -bound of $a \geq 0.26$ and the threshold curve for the GBCS case (see Fig. 3), which is never found from the instability analysis for slowly rotating black holes.

Acknowledgments

This work was supported by the National Research Foundation of Korea (NRF) grant funded by the Korea government (MOE) (No. NRF-2017R1A2B4002057).

References

- [1] D. D. Doneva and S. S. Yazadjiev, *Phys. Rev. Lett.* **120**, no. 13, 131103 (2018) doi:10.1103/PhysRevLett.120.131103 [arXiv:1711.01187 [gr-qc]].
- [2] H. O. Silva, J. Sakstein, L. Gualtieri, T. P. Sotiriou and E. Berti, *Phys. Rev. Lett.* **120**, no. 13, 131104 (2018) doi:10.1103/PhysRevLett.120.131104 [arXiv:1711.02080 [gr-qc]].
- [3] G. Antoniou, A. Bakopoulos and P. Kanti, *Phys. Rev. Lett.* **120**, no. 13, 131102 (2018) doi:10.1103/PhysRevLett.120.131102 [arXiv:1711.03390 [hep-th]].
- [4] C. A. R. Herdeiro, E. Radu, N. Sanchis-Gual and J. A. Font, *Phys. Rev. Lett.* **121**, no. 10, 101102 (2018) doi:10.1103/PhysRevLett.121.101102 [arXiv:1806.05190 [gr-qc]].
- [5] D. C. Zou and Y. S. Myung, *Phys. Rev. D* **102**, no. 6, 064011 (2020) doi:10.1103/PhysRevD.102.064011 [arXiv:2005.06677 [gr-qc]].
- [6] P. V. P. Cunha, C. A. R. Herdeiro and E. Radu, *Phys. Rev. Lett.* **123**, no. 1, 011101 (2019) doi:10.1103/PhysRevLett.123.011101 [arXiv:1904.09997 [gr-qc]].
- [7] L. G. Collodel, B. Kleihaus, J. Kunz and E. Berti, *Class. Quant. Grav.* **37**, no. 7, 075018 (2020) doi:10.1088/1361-6382/ab74f9 [arXiv:1912.05382 [gr-qc]].
- [8] A. Dima, E. Barausse, N. Franchini and T. P. Sotiriou, *Phys. Rev. Lett.* **125**, no. 23, 231101 (2020) doi:10.1103/PhysRevLett.125.231101 [arXiv:2006.03095 [gr-qc]].
- [9] S. Hod, *Phys. Rev. D* **102**, no. 8, 084060 (2020) doi:10.1103/PhysRevD.102.084060 [arXiv:2006.09399 [gr-qc]].
- [10] D. D. Doneva, L. G. Collodel, C. J. Krüger and S. S. Yazadjiev, *Phys. Rev. D* **102**, no. 10, 104027 (2020) doi:10.1103/PhysRevD.102.104027 [arXiv:2008.07391 [gr-qc]].
- [11] C. A. R. Herdeiro, E. Radu, H. O. Silva, T. P. Sotiriou and N. Yunes, *Phys. Rev. Lett.* **126**, no. 1, 011103 (2021) doi:10.1103/PhysRevLett.126.011103 [arXiv:2009.03904 [gr-qc]].
- [12] E. Berti, L. G. Collodel, B. Kleihaus and J. Kunz, *Phys. Rev. Lett.* **126**, no. 1, 011104 (2021) doi:10.1103/PhysRevLett.126.011104 [arXiv:2009.03905 [gr-qc]].

- [13] Y. S. Myung and D. C. Zou, Phys. Lett. B **814**, 136081 (2021) doi:10.1016/j.physletb.2021.136081 [arXiv:2012.02375 [gr-qc]].
- [14] Y. S. Myung and D. C. Zou, arXiv:2103.06449 [gr-qc].
- [15] S. Chandrasekhar, *The Mathematical Theory of Black Holes* (Oxford University Press, New York, 1983).
- [16] Y. S. Myung, Phys. Rev. D **88**, no. 10, 104017 (2013) doi:10.1103/PhysRevD.88.104017 [arXiv:1309.3346 [gr-qc]].
- [17] T. J. M. Zouros and D. M. Eardley, Annals Phys. **118**, 139 (1979). doi:10.1016/0003-4916(79)90237-9
- [18] I. Racz and G. Z. Toth, Class. Quant. Grav. **28**, 195003 (2011) doi:10.1088/0264-9381/28/19/195003 [arXiv:1104.4199 [gr-qc]].
- [19] Y. X. Gao, Y. Huang and D. J. Liu, Phys. Rev. D **99**, no. 4, 044020 (2019) doi:10.1103/PhysRevD.99.044020 [arXiv:1808.01433 [gr-qc]].
- [20] S. J. Zhang, B. Wang, A. Wang and J. F. Saavedra, Phys. Rev. D **102**, no. 12, 124056 (2020) doi:10.1103/PhysRevD.102.124056 [arXiv:2010.05092 [gr-qc]].